Bull. Chem. Soc. Ethiop. **2021**, 35(2), 315-335.
DOI: https://dx.doi.org/10.4314/bcse.v35i2.8

ISSN 1011-3924
Printed in Ethiopia
Online ISSN 1726-801X

SYNTHESIS, STRUCTURAL CHARACTERIZATION AND NEMATICIDAL STUDIES OF SOME NEW N_2O_2 SCHIFF BASE METAL COMPLEXES

Sherif M. Abd El-Hamid[1*], Sadeek A. Sadeek[2], Ahmed F. El-Farargy[2] and Nosa S. Abd El-Lattif[3]

[1]Department of Basic Science, Higher Future Institute of Engineering and Technology, Mansoura, Egypt
[2]Department of Chemistry, Faculty of Science, Zagazig University, Zagazig, Egypt
[3]Department of Pesticides Formulation, Central Agricultural Pesticides Laboratory, Cairo, Egypt

(Received December 21, 2020; Revised April 19, 2021; Accepted May 3, 2021)

ABSTRACT. Cobalt(II), copper(II), yttrium(III), zirconium(IV), lanthanum(III) and uranium(VI) complexes of 1,4-di(2-hydroxybenzylidene)thiosemicarbazide (H_2L) were prepared and characterized. The proposed structures were determined from their elemental analyses, molar conductivities, magnetic moment, IR, Proton NMR, UV-Vis., mass spectra, X-ray diffraction and thermal analyses measurements. The high conductance data supply evidence for the electrolytic nature of the complexes. The changes in the selected bands in IR of Schiff base ligand upon coordination showed that Schiff base exhibits as a neutral tetradentate manner with oxygen and nitrogen donor sites. The complexes are thermally steady at room temperature and break up to two or three steps. The kinetic and thermodynamic parameters of complexes have been determined by using Coats-Redfern and Horowitz-Metzeger methods at n=1 and n≠1 and values suggest more ordered activated complex formation. The calculated bond length and force constant, F(U=O), in the uranyl complex are 1.744 Å and 664.886 Nm^{-1}. The nematicidal activity of free Schiff base and all complexes were investigated and showed a low inhibition percentage (%I) of complexes compared with H_2L.

KEY WORDS: Schiff base, IR, Thermal, XRD, Nematicidal activity

INTRODUCTION

In recent year, agricultural plant diseases and insect pests are becoming more severe in the world [1-4]. So, discovery of agrochemicals (fungicide, insecticide and nematicide) is facing with enormous challenges [5]. Plant parasitic nematodes are the main pathogens on most fiber crops, horticultural, food and vegetable crops and without adequate control; they cause loss of yield and quality. Nematode *Meloidogyne* species is known to attack almost all types of plants and cause considerable damage [6]. The past literature works concerning nematode problems have indicated that some Schiff bases and their metal complexes act as active nematicidal agents [7, 8].

Schiff bases compounds were easily prepared by the condensation reaction of primary amines with carbonyl compounds (aldehyde/ketone) and are most widely used as chelating ligands in coordination chemistry [9-11]. Tetradentate Schiff bases containing nitrogen and oxygen donor atoms are well known for their coordination with various metal ions, forming stable compounds and make significant contributions to biological systems [12-14].

The Cu(II) complex ($C_{15}H_{11}N_3O_2SCu$) was prepared with new Schiff base ligand H_2L ($C_{15}H_{11}N_3O_2S$). The ligand and the complex were isolated from the reaction in the solid form and characterized by IR, UV-visible, ^1H NMR, thermal analysis and some physical measurements. Spectroscopic evidence indicated that the Schiff base was behaved as N,O coordinating chelating agents. The Schiff base and its Cu(II) complex have been shown moderate to strong antimicrobial activity [15]. The literature survey indicates no work on H_2L against nematicidal activity.

*Corresponding author. E-mail: sherifmohamed266@gmail.com

The aim of this work was focused to study the synthesis and characterization of 1,4-di(2-hydroxybenzylidene)thiosemicarbazide (H_2L) (Scheme 1) Schiff base complexes with Co(II), Cu(II), Y(III), Zr(IV), La(III) and U(VI) in order to determine the site and kind of donation and the effect of atomic volume and oxidation state of the metal ions on nematicidal activity of H_2L. All the compounds were characterized using melting point, elemental analysis, molar conductivity, IR, Ultraviolet-Visible, Proton NMR, mass spectra, XRD as well as thermal analysis. The kinetic parameters for compounds were counted. Also, activity of the investigated compounds against nematicidal were evaluated.

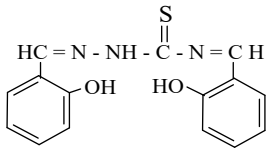

Scheme 1. 1,4-Di(2-hydroxybenzylidene)thiosemicarbazide (H_2L).

EXPERIMENTAL

Chemicals

All chemicals used for the synthesis of compounds were of the analytical reagent grade, commercially available from various sources with highest purity. Salicylaldehyde, glacial acetic acid, absolute ethanol, $FeCl_3.6H_2O$, $ZrOCl_2.8H_2O$ (99.9%), $AgNO_3$, thiosemicarbazide were purchased from Fluka Chemical Co. $CoCl_2.6H_2O$, $Cu(CH_3COO)_2$, $YCl_3.6H_2O$, $LaCl_3.7H_2O$ and $UO_2(CH_3COO)_2.2H_2O$ from Aldrich Chemical Co.

Synthesis of 1,4-di(2-hydroxybenzylidene)thiosemicarbazide Schiff base ($C_{15}H_{13}N_3SO_2$) H_2L

The Schiff base was synthesized by mixing an ethanolic solution of thiosemicarbazide 1 mmoL (0.091 g) with salicylaldehyde 2 mmoL (0.244 mL) into a two necked round bottomed flask equipped with a magnetic stirrer. The reaction mixture was boiled under reflux for 10 h and the mixture was concentrated to 8 mL on a water bath and allowed to cool at 0 °C. Light yellow precipitate was filtered off, washed several times by ethanol and dried under vacuum over $CaCl_2$.

Synthesis of metal solid complexes

The black solid complex $[Co(H_2L)(H_2O)_2]Cl_2{\cdot}2H_2O$ **(A)** was prepared by adding 1 mmoL (0.238 g) of cobalt chloride hexahydrate in 30 mL absolute ethanol drop-wisely to a stirred solution 1 mmoL (0.299 g) of H_2L in 30 mL ethanol. The reaction mixture was boiled and stirred under reflux for 12 h. The black precipitate was filtered off, washed several times by ethanol and dried under vacuum over anhydrous $CaCl_2$. The gray, yellow, orange, yellow and dark orange solid complexes of $[Cu(H_2L)(H_2O)_2](CH_3COO)_2$ **(B)**, $[Y(H_2L)(H_2O)_2]Cl_3{\cdot}9H_2O$ **(C)**, $[ZrO(H_2L)(H_2O)]Cl_2{\cdot}7H_2O$ **(D)**, $[La(H_2L)(H_2O)_2]Cl_3.8H_2O$ **(E)** and $[UO_2(H_2L)](CH_3COO)_2.6H_2O$ **(F)** were prepared in a similar manner described above by using ethanol as solvent.

The chemical name of the prepared complexes were written as the following $[Co(H_2L)(H_2O)_2]Cl_2{\cdot}2H_2O$ complex, 1,4-di(2-hydroxybenzylidene)thiosemicarbazide diaqua cobalt chloride dehydrate, $[Cu(H_2L)(H_2O)_2](CH_3COO)_2$ complex, 1,4-di(2-hydroxy-benzylidene)thiosemicarbazide diaqua copper acetate, $[Y(H_2L)(H_2O)_2]Cl_3{\cdot}9H_2O$, 1,4-di(2-

hydroxybenzylidene)thiosemicarbazide diaqua yttrium chloride nonahydrate, $[ZrO(H_2L)(H_2O)]Cl_2{\cdot}7H_2O$, 1,4-di(2-hydroxybenzylidene)thiosemicarbazide oxoaqua zirconium chloride heptahydrate, $[La(H_2L)(H_2O)_2]Cl_3.8H_2O$, 1,4-di(2-hydroxybenzylidene) thiosemicarbazide diaqua lanthanum chloride octahydrate, $[UO_2(H_2L)](CH_3COO)_2.6H_2O$, 1,4-di(2-hydroxybenzylidene)thiosemicarbazide dioxouranium acetate hexahydrate.

Instruments

Carbon, hydrogen and nitrogen contents were determined on a Perkin Elmer CHN 2400. The percent of the metal ions were identified gravimetrically by conversion the solid products into metal or metal oxide and also identified by using atomic absorption method. Spectrometer model PYE-UNICAM SP 1900 supplied with the corresponding lamp was used for this work. Fourier transform-IR spectra in KBr discs were recorded in the range from 4000-400 cm^{-1} with FT-IR 460 PLUS Spectrophotometer, Proton NMR spectra were recorded on Varian Mercury VX-300 NMR Spectrometer using dimethyl sulfoxide-d_6 as solvent. TG-DTG measurements were done under N_2 atmosphere within the temperature range from room temperature to 1000 ^oC using TGA-50H Shimadzu, the mass of sample was accurately weighted out in an aluminum crucible. Electronic spectra were done using UV-3101PC Shimadzu. The absorption spectra were recorded as solutions in DMSO-d_6 using UV-3101PC Shimadzu. Mass spectra were recorded on GCMS-QP-1000 EX Shimadzu (ESI-70 eV) in the range from 0-1090. XRD analyses were carried out by using a Philips Analytical X-ray BV, diffractometer type PW 1840. Radiation was provided by a copper target (Cu anode 2,000 W) high intensity X-ray tube operated at 40 kV and 25 mA. Magnetic susceptibilities of the complexes were carried out on a Sherwood scientific magnetic balance using Gouy balance at room temperature using mercury(II) tetrathiocyanatocobaltate(II) as calibrant. The molar conductance of 1×10^{-3} M solutions of the ligands and their complexes in dimethylformamide was done at room temperature using CONSORT K410. Melting points were recorded by a Buchi apparatus. All measurements were done with new prepared solutions at room temperature.

Nematicidal investigation (culture technique)

Nematicidal activity of the ligand and its metal complexes was investigated [16]. Root-Knot nematode (*Meloidgyne javanica*) propagated in pure culture in central Agricultural Pesticides Laboratory. Individual egg-masses with their mature females were removed from galls of the infected roots. Each egg-mass was placed in 10 mL glass capsule containing distilled water. The female under the particular egg-mass was removed from root tissue, dissected and identified by microscope examination of its perineal pattern system. Identification was recorded according to its corresponding egg-mass of previously identified females. Egg-mass were singly put on root system of two weeks old tomato seedling race number (CV). Pritchard in 15 cm clay pots filled with steam sterilized sandy loam soil. The inoculated pots were watered thoroughly and kept in greenhouse at 25±5 °C. Two months after inoculation the plants were removed from the pots and the root system of each plant was examined for nematodes infection and reproduction. Samples were from the infected roots which contained adult females and egg-masses for identification to confirm the nematode species to their original patterns. The infected roots were used for inoculation of tomato seed lings CV. Pritchard growth in 25 cm pots filled with 3:1 mixture of sandy:clay soil. New tomato seedlings were transplanted to the pots as needed. By repeating this procedure enough quantities of inocula from pure culture were obtained.

Bioassay technique

Evaluation of tested ligand and its complexes as nematicides were carried out according to migration method [16]. Bioassay unit consists of polyethylene tube of 1.3 cm long and 2.4 cm

diameter covered at one end with two layers, the first one is paper handkerchief then muslin cloth. It filled with washed air-dried sand of particle size 250 µ and placed upright in a Petri-dish 5 cm diameter serial concentration from tested ligand and its complexes were prepared in ethanol. 1 mL of tested concentration was pipetted on surface of sand in each tube and kept at 25±5 °C to evaporate the solvent. After 24 h, 1 mL of water was pipetted on surface of sand in each tube, then 1 mL of nematode suspension containing 100 second stage larvae of *M. javanica* was pipetted on the surface of the sand in each tube. Each bioassay unit was transferred to Petri dish (9 cm diam) containing filter paper saturated with 2 mL water to serve as humidity room to prevent evaporation. After 24 h the bioassay unit took up from humidity room and 8 mL distilled water was added in Petri dish of bioassay unit. The number of second stage larvae that had migrated in bioassay dish was recorded 72 h later. The number of migrated second stage larvae in treatments was expressed as percentage of number in control and each treatment was replicated four times. The percentages of inhibition were established.

RESULTS AND DISCUSSION

The Schiff base (H_2L) reacts with Co(II),Cu(II), Y(III), Zr(IV), La(III) and U(VI) in ethanol to form solid complexes. The complexes were obtained as colored powdered materials and characterized using elemental analysis, molar conductivity, magnetic susceptibility, melting point, IR, mass, UV-Vis, ^{1}H NMR spectra, XRD and thermogravimetric analyses. The molar ratio for all synthesized complexes is H_2L:M = 1:1 which was established from the results of the chemical analyses (Table 1) and also all the prepared complexes have water molecules and the number of binding water molecules in these complexes being different. The elemental analyses agree with the chemical formulas of compounds. The infrared spectra and thermal analysis proved that presence of water molecules in the composition of the complexes. The metal ions are coordinated with the two phenolic oxygen and two nitrogen atoms of H_2L to form chelating six and five membered rings and complete the coordination number with one or two water molecules.

Table 1. Elemental analysis and physico-analytical data for H_2L and its metal complexes.

Compounds F.Wt. (M.F.)	Yield %	M.p. °C	Color	Found (calcd.) (%)						Λ, S cm^2 mol^{-1}
				C	H	N	S	Cl	M	
H_2L 299 ($C_{15}H_{13}N_3SO_2$)	90	225	Yellow	60.10 (60.20)	4.32 (4.35)	14.01 (14.05)	10.46 (10.70)	-	-	10.00
(A) 500.893 ($CoC_{15}H_{21}Cl_2N_3SO_6$)	80	>300	Black	35.91 (35.94)	4.17 (4.19)	8.36 (8.39)	6.35 (6.39)	14.15 (14.17)	11.74 (11.77)	194.11
(B) 516.546 ($CuC_{19}H_{23}N_3SO_8$)	70	>300	Gray	44.11 (44.14)	4.43 (4.45)	8.11 (8.13)	6.16 (6.19)	-	12.26 (12.30)	169.15
(C) 692.4 ($YC_{15}H_{35}N_3\ Cl_3SO_{13}$)	75	>300	Yellow	25.98 (26.00)	5.04 (5.05)	6.05 (6.07)	4.60 (4.62)	15.35 (15.38)	12.81 (12.84)	275.10
(D) 621.22 ($ZrC_{15}H_{29}Cl_2N_3SO_{11}$)	80	>300	Orange	28.88 (28.98)	4.57 (4.67)	6.74 (6.76)	5.12 (5.15)	11.39 (11.43)	14.58 (14.68)	190.15
(E) 724.4 ($LaC_{15}H_{33}N_3\ Cl_3SO_{12}$)	70	>300	Yellow	24.75 (24.85)	4.50 (4.56)	5.78 (5.80)	4.40 (4.42)	14.66 (14.70)	19.15 (19.18)	270.09
(F) 795 ($UC_{19}H_{31}N_3SO_{14}$)	75	210	Dark Orange	28.58 (28.68)	3.86 (3.90)	5.25 (5.28)	4.00 (4.03)	-	29.91 (29.94)	165.10

Conductivity measurements

Conductivity measurements have frequently been used in foretells the structural of metal chelates within the limits of their solubility. They provide a method of testing the degree of

ionization of the complexes, the molecular ions that a complex releases in solution, the higher will be its molar conductivity and vice versa [17]. The molar conductance values of H_2L and its metal complexes in DMF with standard reference, using $1x10^{-3}$ M solutions at room temperature were found to be in the range 10.00 to 275.10 S cm^2 mol^{-1} (Table 1). Qualitative reactions also agree well with the molar conductance data which revealed the presence of Cl^- and $(CH_3COO)^-$ ions as counter ions. The complexes solutions were tested with aqueous solutions of $AgNO_3$ and $FeCl_3$ where a white precipitate and red brownish color were formed respectively, which indicated the presence of Cl^- and $(CH_3COO)^-$ out the complex sphere.

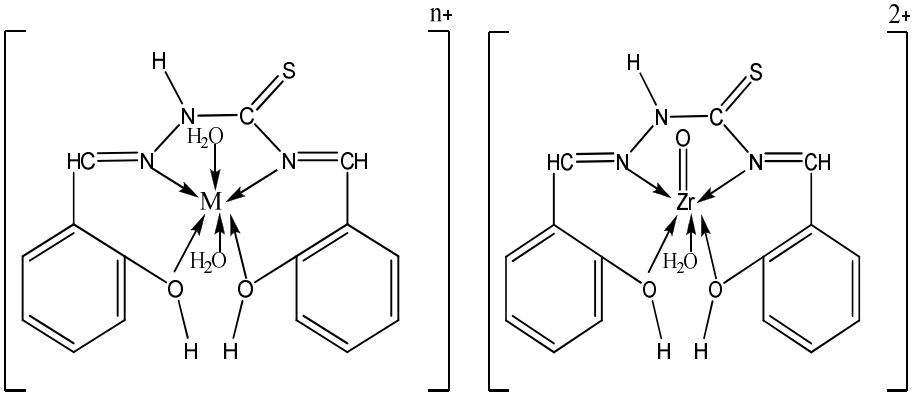

M = Co(II), Cu(II), Y(III) and La(III), n = 2 or 3

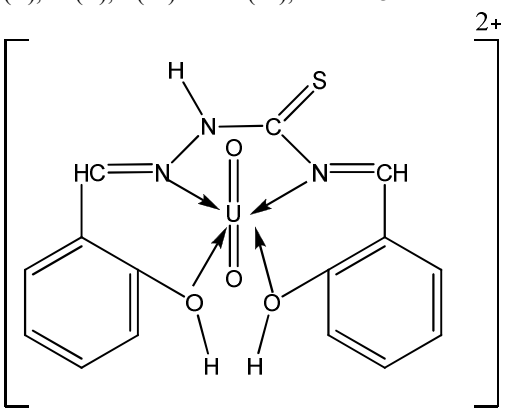

Scheme 2. The coordination mode of Co(II), Cu(II), Y(III), La(III), Zr(IV) and U(VI) with H_2L.

IR absorption spectra

The infrared spectra of the complexes are compared with those of the free H_2L in order to determine the coordination sites that may be involved in chelation (Figure 1). There are some guide peaks in the spectrum of H_2L, which are of good help for obtaining this goal. These peaks are prospective to be involved in chelation. The position and/or the intensities of these peaks are prospective to be changed upon complexation. New peaks are also guide peaks as well as water of crystallization or coordinated. The IR of the free H_2L does not display the ν(S-H) at 2550 cm^{-1} pointing that, free ligand found in thione tautomer in the solid state form [18, 19]. The presence of the spectral absorption band at around 3435 cm^{-1} in all complexes may be assigned

to *ν*(O-H) vibration of phenolic group and water molecules [20, 21]. The ν(N-H) bands occurred in compounds at around 3308 cm^{-1}. The bands observed at 1610 and 1537 cm^{-1} in the spectrum of the H_2L have been assigned to the stretching vibration of azomethine groups ν(C=N) [22, 23]. The shift of ν(C=N) to a lower wave number (around 1540 and 1480 cm^{-1}) indicating the participation of azomethine group of H_2L in coordination to the metal ion and the electron density on the nitrogen atom reduced [24, 25]. The coordination of the metal ions via oxygen and nitrogen of H_2L is also confirmed by ν(M-O) and ν(M-N). The ν(M-O) and ν(M-N) bands observed at 597 and 492 cm^{-1} for Co(II), 593 and 474 cm^{-1} for Cu(II), 523 and 469 cm^{-1} for Y(III), 645 and 485 cm^{-1} for Zr(IV), 527 and 469 cm^{-1} for La(III) and 562 and 451 cm^{-1} for U(VI), which are absent in the spectrum of H_2L. Therefore, from the infrared spectra, it is concluded that the H_2L behave as tetradentate ligand through oxygen of phenolic group and nitrogen of C=N donor sites involved in the coordination sphere. The proposed structures for complexes are represented in Scheme 2 and the ν(Zr=O) found as a medium band at 878 cm^{-1}. for U(VI), the ν_{as}(U=O) occurs at 948 cm^{-1} as a medium singlet and ν_s(U=O) is observed at 829 cm^{-1} [26, 27]. The ν(U=O) of the uranyl unit in the complex occurs at lower frequency values compatible with those for the same unit, UO_2, in simple salt. the ν_s(U=O) value was used to counted both the bond length and the bond stretching force constant, f(U=O), for uo_2 bond in (f) complex [28, 29]. The calculated bond length and force constant values are 1.744 å and 664.886 nm^{-1}, respectively.

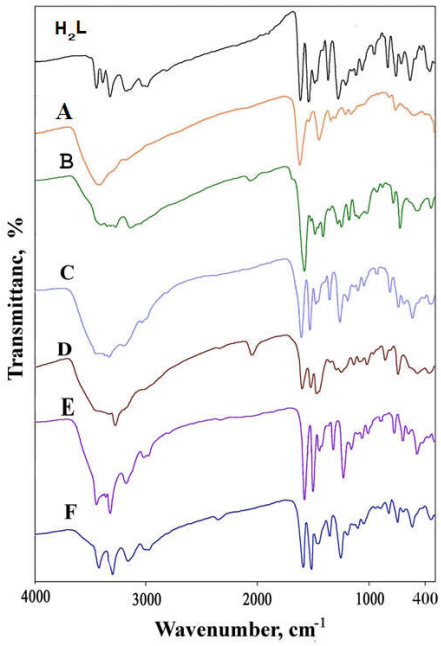

Figure 1. Infrared spectra for H_2L and its metal complexes.

Magnetic measurements and electronic spectra

The magnetic moments (as B.M.) of the complexes were predestined at room temperature. The complexes **(A)** and **(B)** are found in paramagnetism with measured magnetic moment values at 5.11 and 2.25 B.M., respectively, and the other complexes **(C)**, **(D)**, **(E)** and **(F)** found as diamagnetism. The application of ultraviolet spectroscopy is more universal and can be useful in structural determinations of all chelates since they all absorb in this region [30]. The formation of

the metal ligand complexes was also assured by the absorption spectra. The electronic absorption spectra of H_2L along with the **(A)**, **(B)**, **(C)**, **(D)**, **(E)** and **(F)** complexes in the wavelength interval from 200 to 800 nm ranges (Figure 2). It can be seen that H_2L reflected at 240, 301 and 351 nm. The first band at 240 nm may be attributed to π-π^* transition and the second two bands observed at 301 and 351 nm are assigned to n-π^* transitions, within the C=N and C=S bonds which influenced by charge transfer interaction [31]. The shift of bands to higher (bathochromic shift) or lower (hypsochromic shift) values denote the formation of their metal complexes. The complexes have bands in the range from 500 to 570 nm, which may be denoted by the ligand to metal charge-transfer [32]. The electronic absorption spectral band of Co(II) complex, give band at 690 nm., the band is assigned to $^4T_{1g}(F)\rightarrow{}^4T_{1g}(P)$ transition typified octahedral geometry [33] with magnetic moment value 5.11 B.M. which indicated high spin nature of the complex with three unpaired electrons. For gray Cu(II) complex have band 630 nm, which may be assigned to $^2B_{1g}\rightarrow{}^2E_g$ transition [34]. The magnetic moment value is 2.25 B.M. in favor of octahedral geometry.

The ^1H NMR spectra

The formation of the metal complexes was also assured by proton NMR spectra. ^1H NMR spectra of H_2L and its complexes were done in DMSO- d_6 as a solvent (Figure 3). The ^1H NMR spectrum of H_2L showed singlet at δ: 6.79–6.88 ppm corresponding to -CH aliphatic, doublet at δ: 7.18–7.20 ppm 0.02 (d, J = 6.00 Hz, C-H (3,6), (3",6"), 4H) for –CH aromatic and triplet at 7.66-8.37 ppm for –CH aromatic, singlet at δ: 2.49–2.51 ppm corresponding to -NH of amide group and singlet at δ:around 9.96 and 11.34 ppm corresponding to –OH. Also, the ^1H NMR spectra for complexes exhibit new peak in the range 3.31–3.77 ppm, due to the presence of water molecules in the complexes. On comparing main peaks of free ligand with its complexes, it is observed that all the peaks of the free ligand are present in the spectra of the complexes with chemical shift upon binding of free ligand to the metal ion [35]. In order to make sure for the presence of the two protons of –OH in all complexes, the spectrum of U(VI) complex as an example was done in presence of D_2O which indicated the presence of the –OH protons in the complex.

Mass spectra

Mass spectrometry was found useful as a complementary tool. The stability of complexes under conditions are dependent on different factors such as counter ions, the ligand itself, solvent, the metal ion, temperature, concentration, etc. The electron impact spectra of the prepared complexes are registered and investigated at 70 eV. The mass spectra of the compounds H_2L, **(A)**, **(B)**, **(C)**, **(D)**, **(E)** and **(F)** displayed molecular peaks at 299, 499, 516, 690, 620, 722 and 795, respectively, which refer to M.W. of these complexes and the fragmentation models of our studied complexes were obtained from the mass spectra (Figure 4). Mass spectrum of the synthesized H_2L is in a good agreement with the suggested formula. The H_2L showed molecular peak (M^+) at m/z = 299 (80 %) (Scheme 3). The molecular ion peak [a] loses C_6H_5O gave fragment which refer to base peak [b] at m/z = 206 (60%). The molecular ion peak [a] loses C_7H_6ON to give fragment [c] at m/z = 179 (50%) and it loses C_8H_6NOS to give fragment [d] at m/z = 135 (45%). It loses CS to give [e] at m/z = 255 (20%). The molecular ion peak [a] give fragment [f] at m/z = 113 (70%) when loses $C_{12}H_{10}O_2$. The fragmentation patterns of our studied complexes were obtained from mass spectra. The mass spectrum of complex **(B)** displayed molecular peak at m/z = 516 (90%) (Scheme 4) suggesting that the molecular weight of the assigned product matching with elemental analysis calculated. Fragmentation pattern of the complex **(B)** is given as an example. The molecular ion peak [a] appeared at m/z = 516 (90%) loses $C_4H_6O_4$ to give [b] at m/z = 398 (80%) and it also loses CHNS to give [c] at m/z = 457

(70%). The molecular ion peak [a] loses $C_4H_{10}O_6$ to give [d] at m/z = 362 (60%) and it loses $2C_6H_6O$ to give [e] at m/z = 326 (50%). The molecular ion peak also loses $C_{10}H_{14}O_6$ to give [f] at m/z = 286 (40%) and also loses C_6H_4 to give [g] at m/z = 440 (30%).

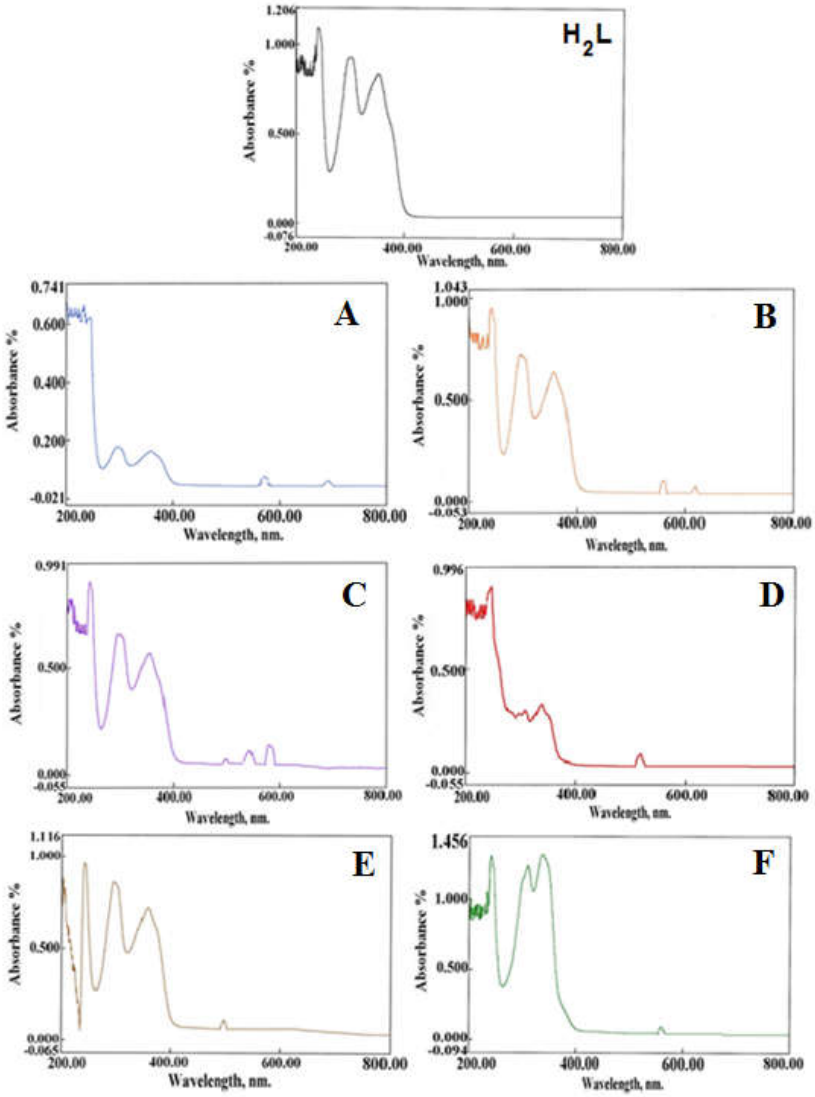

Figure 2. Electronic absorption spectra for H_2L and its metal complexes.

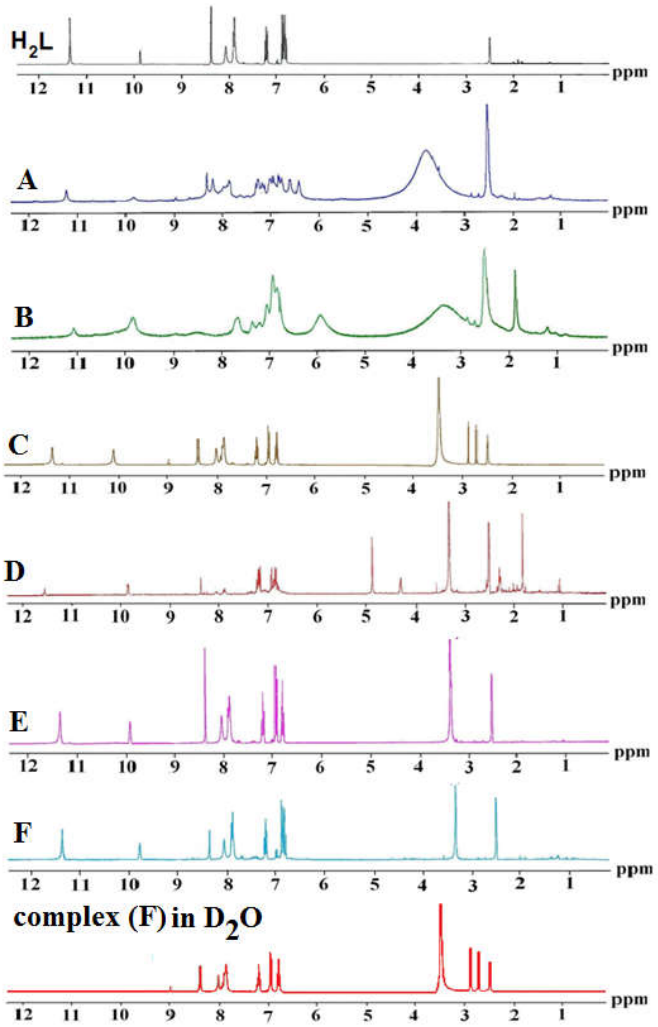

Figure 3. ^{1}H NMR spectra for H_2L and its metal complexes.

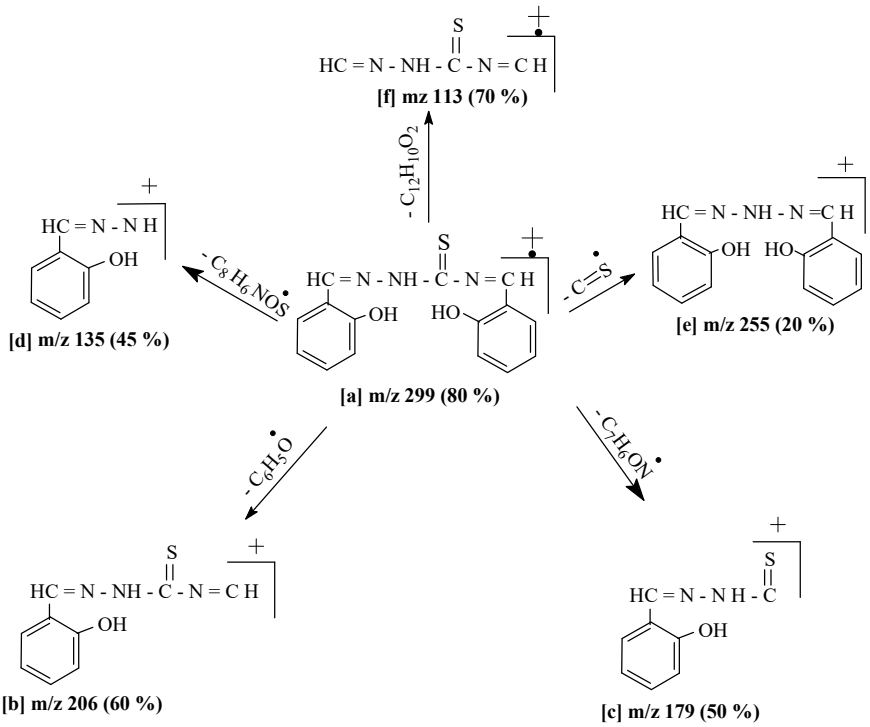

Scheme 3. Fragmentation pattern of H_2L.

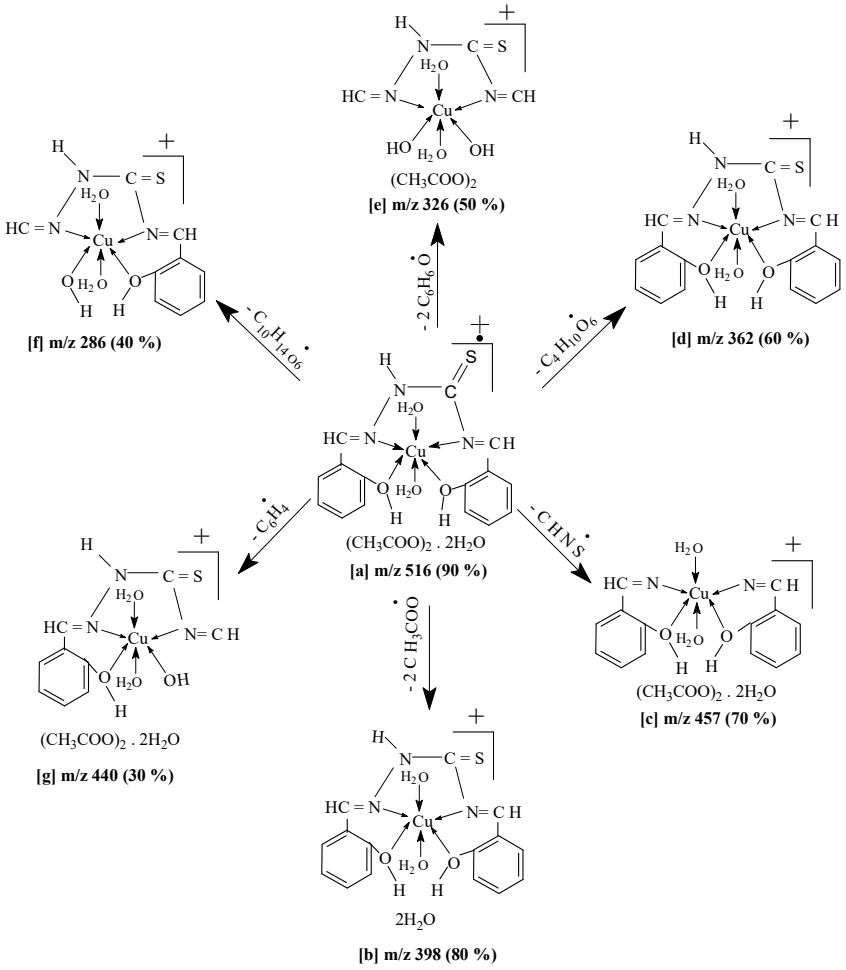

Scheme 4. Fragmentation pattern of complex **(B)**.

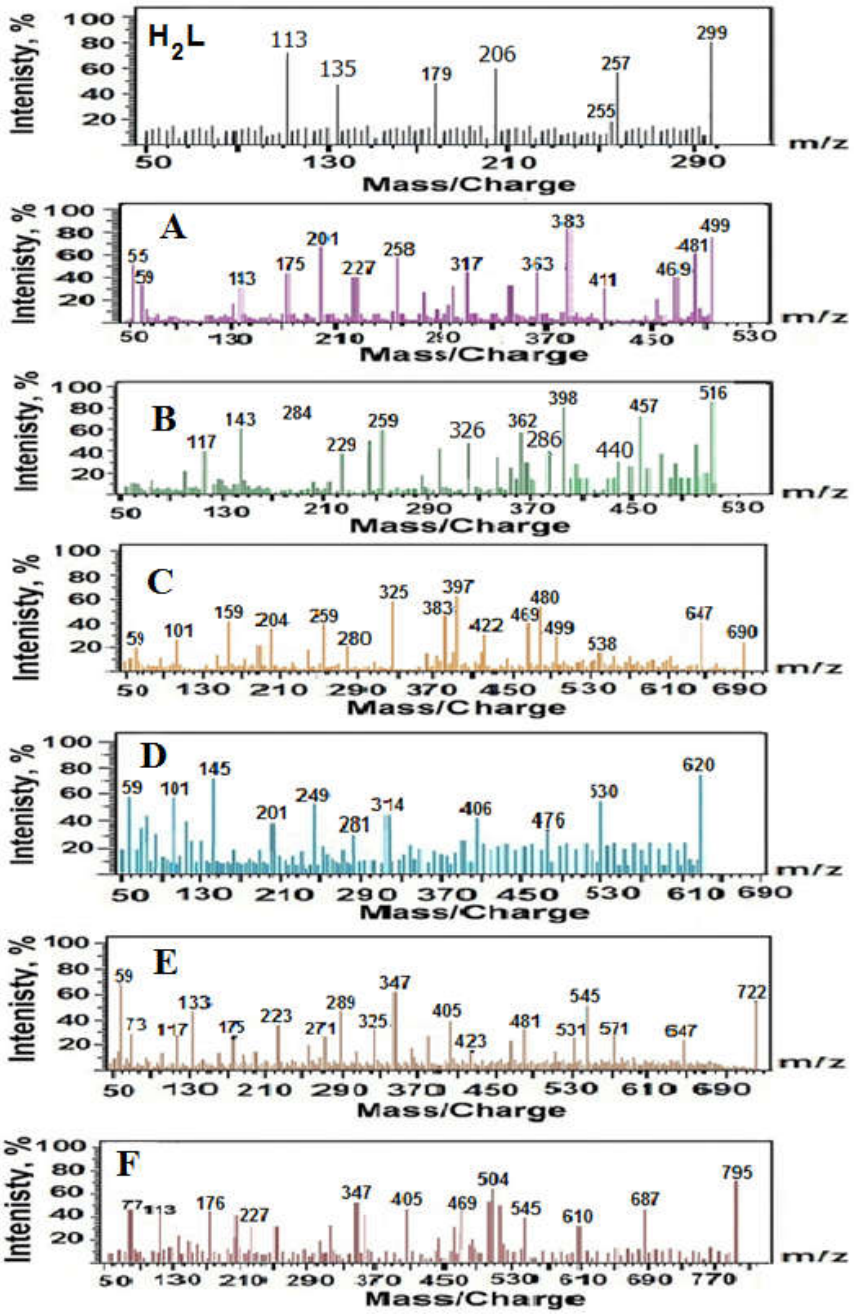

Figure 4. Mass spectra diagrams for H_2L and its metal complexes.

Thermal analyses

Thermogravimetric analyses (TG) and (DTG) of H_2L and its complexes are used to get information about the thermal stability of these new complexes, set whether the water molecules (if present) are inside or outside the inner coordination field of the central metal ion and to propose a general sketch for thermal degradation of these chelates. In the present study, heating ratio was suitably controlled at 10°C/ min. The TG and DTG curve of the compounds are shown in Figure 5. The data support the proposed complexes chemical formulas. Decomposition of H_2L ($C_{15}H_{13}N_3SO_2$) started at room temperature and finished at 600 °C with one stage at two

Table 2. The maximum temperature T_{max} (°C) and weight loss values of the decomposition stage for H_2L and its metal complexes.

Compounds	Decomposition	T_{max}(°C)	Weight loss (%)		Lost species
			Calc.	Found	
H_2L	First step	230,255	100	99.62	$5C_2H_2+C_4H_2+N_2+HCN+SO_2$
($C_{15}H_{13}N_3SO_2$)	Total loss		100	99.62	
	Residue				
(A)	First step	57,129	7.09	7.03	$2H_2O$
($CoC_{15}H_{21}Cl_2N_3SO_6$)	Second step	253	7.10	7.09	$2H_2O$
	Third step	356,466 ,597	71.65	71.82	$2C_4H_2+3HCN+2HCl+2C_2H_2+SO_2$
	Total loss		85.84	85.94	
	Residue		14.16	14.06	CoO
(B)	First step	224	29.81	29.80	$2H_2O+2CO_2+C_2H_6$
($CuC_{19}H_{23}N_3SO_8$)	Second step	338,554	52.46	52.45	$NH_3+N_2O+H_2S+C_2H_2+3C_4H_2$
	Total loss		82.27	82.25	
	Residue		17.72	17.42	CuO+C
(C)	First step	75,120	23.39	23.39	$9H_2O$
($YC_{15}H_{35}N_3Cl_3SO_{13}$)	Second step	227,611	59.14	58.84	$HCN+2CO+0.5H_2+6C_2H_2+2NO+3HCl$
	Total loss				
	Residue		82.54	82.24	
			17.46	17.76	Y+S
(D)	First step	72	5.79	5.79	$2H_2O$
($ZrC_{15}H_{29}Cl_2N_3SO_{11}$)	Second step	231	17.38	17.38	$6H_2O$
	Third step	704,805 ,947	23.17	23.18	$2CNCl+0.5H_2+0.5N_2+3CO+5C_2H_2+H_2S$
	Total loss		62.13	62.13	
	Residue		14.68	14.68	Zr
(E)	First step	59,84,140	19.87	19.74	$8H_2O$
($LaC_{15}H_{33}N_3Cl_3SO_{12}$)	Second step	235	5.00	4.99	$2H_2O$
	Third step	597	52.64	52.87	$6C_2H_2+HCN+Cl_2+SO_2+N_2$
	Total loss		77.51	77.60	
	Residue		22.49	22.40	La+2C
(F)	First step	220	28.42	29.00	$6H_2O+2CO_2+C_2H_6$
($UC_{19}H_{31}N_3SO_{14}$)	Second step	535,759	37.61	37.04	$2CO+HSCN+2HCN+5C_2H_2$
	Total loss		66.03	66.04	
	Residue		33.96	33.96	UO_2

maxima 230 and 255 °C with a weight loss 99.62%, corresponding exactly to the loss of $5C_2H_2+C_4H_2+N_2+HCN+SO_2$. The TG curve of complex **(A)** exhibits three main degradation steps (Table 2). The first step occurred in the range 20-179 °C at two maxima 57 and 129 °C with a weight loss of 7.09%, which may be due to elimination of lattice water. The second step of degradation occurred at one maximum 253 °C with a weight loss of 7.10%, corresponding to

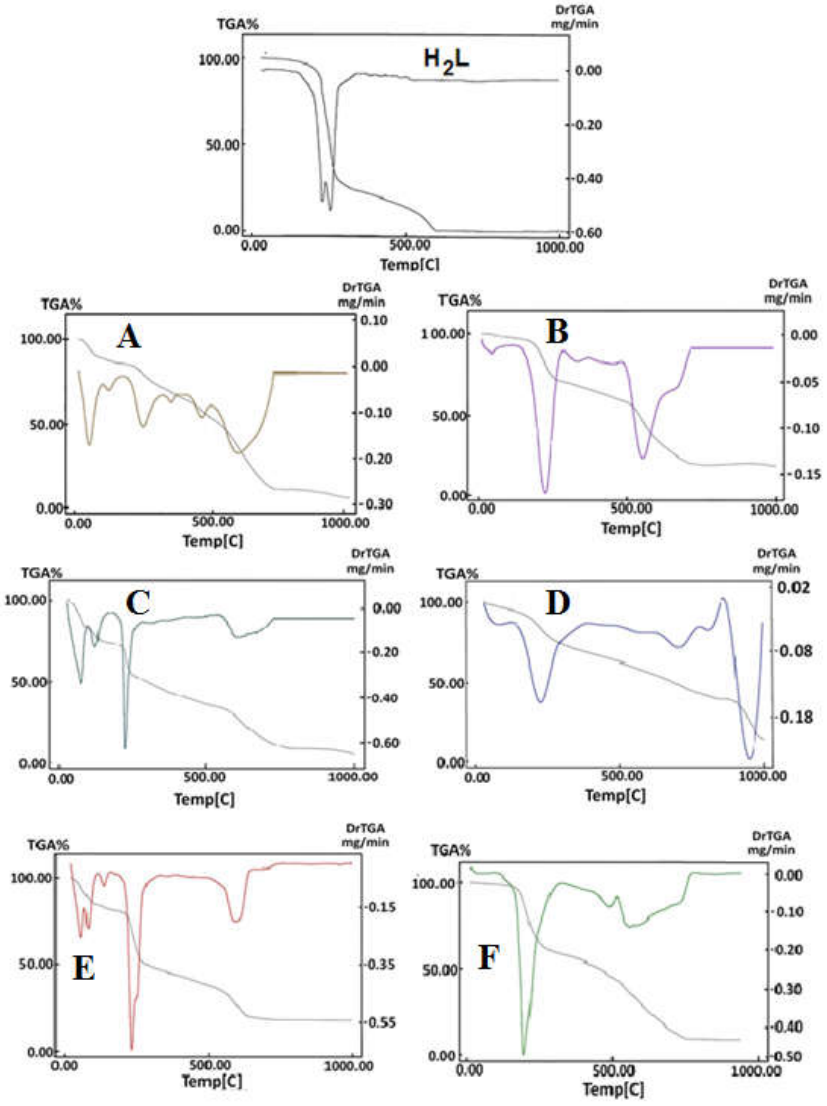

Figure 5. TGA and DTG diagrams for $\mathbf{H_2L}$ and its metal complexes.

the loss of the two coordinated water molecules. The third step occurred at three maxima 356, 466 and 597 °C with a weight loss 71.82%, corresponding exactly to the loss of $2C_4H_2$+3HCN+2HCl+$2C_2H_2$+SO_2 giving CoO (14.06%) as a final product. The TG curves of complexes **(B)** and **(C)** exhibit two main degradation steps. The first step occurred in the range 25-292 °C and 25-151 °C, respectively, and accompanied by a weight loss of 29.81% and 23.397%. The second step found at 338, 554 °C and 227, 611 °C maxima, respectively, and

accompanied by a weight loss of 52.46%, and 59.14% corresponding to the loss of NH_3+N_2O+H_2S+C_2H_2+$3C_4H_2$ and HCN+2CO+$0.5H_2$+$6C_2H_2$+2NO+3HCl giving CuO+C and Y+S as a thermally stable final products. Thermogravimetric for complexes **(D)** and **(E)** show three weight loss events. The first step of decomposition occurred in the range 40-150 °C and 25-161 °C with maxima temperatures at 72 °C and 59, 84, 140 °C, respectively, corresponding to the loss of two and eight hydrated water molecules. The second step of decomposition occurs in at 231 °C and 235 °C. The third step of decomposition occurred at three maxima for complex **(D)** 704, 805, 947 °C and at one maximum 597 °C for complex **(E)** corresponds to the loss of 2CNCl+$0.5H_2$+$0.5N_2$+3CO+$5C_2H_2$+H_2S and $6C_2H_2$+HCN+Cl_2+SO_2+N_2, respectivly, giving Zr metal and La+2C as a final products. The thermal decomposition of complex **(F)** proceeds with two degradation steps. The first step occurred at 220 °C maximum temperatures with loss of $6H_2O$+$2CO_2$+C_2H_6. The second step found at 535 and 759 °C maxima and is simultaneously decomposed to oxide with intermediate formation of very unstable products which were not identified [36] and is accompanied by a weight loss of 37.61%, corresponding to the loss of 2CO+HSCN+2HCN+$5C_2H_2$. The actual weight loss from these two steps is 66.04%, close to the calculated value 66.038%, giving UO_2 as a final product. Loss of water of crystallization for the complexes at a relatively low temperature may indicate weak H-bonding involving the H_2O molecule and the complexes. The decomposition mechanisms are only based on speculation and the thermal analysis without a complementary technique (gas chromatography). The suggested residues confirmed on the basis weight loss % calculation and IR for final product.

Table 3. Thermal behavior and kinetic parameters determined using the Coats–Redfern (CR) and Horowitz–Metzger (HM) operated for H_2L and its metal complexes.

Compounds	Decomposition range (K)	T_s (K)	Method	Parameter					R^a	SD^b
				E^* (kJ/ mol)	A (s^{-1})	ΔS^* (kJ/mol.K)	ΔH^* (kJ/mol)	ΔG^* (kJ/mol)		
H_2L	500-592	529	CR	166.89	2.6×10^{14}	0.02621	162.49	148.63	0.995	0.05
			HM	175.31	2.6×10^{15}	0.04532	170.91	146.94	0.995	0.11
(A)	293-364	330	CR	15.03	0.33	-0.255	12.29	96.4	0.9996	0.01
			HM	19.14	3.8	-0.235	16.40	93.8	0.998	0.03
	453-568	525	CR	106.8	1.8×10^{8}	-0.092	102.42	150.49	0.99	0.13
			HM	115.2	2.5×10^{9}	-0.070	110.87	147.55	0.99	0.15
(B)	332-565	497	CR	53.32	1.25×10^{3}	-0.1898	49.19	143.543	0.99	0.13
			HM	66.85	5.76×10^{4}	-0.1580	62.71	141.25	0.997	0.09
	749-1034	827	CR	125.25	4.46×10^{5}	-0.1452	118.37	238.49	0.985	0.18
			HM	125.84	3.27×10^{5}	-0.1478	118.96	241.20	0.987	0.19
(C)	296-364	348	CR	33.02	3.63×10^{2}	-0.1972	30.12	98.74	0.989	0.14
			HM	39.18	4.93×10^{3}	-0.1755	36.28	97.36	0.99	0.12
	425-533	500	CR	177.05	2.80×10^{16}	0.0657	172.90	140.07	0.976	0.22
			HM	183.61	1.122×10^{20}	0.1346	179.46	112.15	0.999	0.04
(D)	418-851	504	CR	35.41	3.69	-0.2384	31.22	151.39	0.98	0.13
			HM	43.95	14.98	-0.2268	39.76	154.05	0.98	0.16
	1119-1272	1220	CR	228.31	1.3015	-0.0629	218.16	295.02	0.995	0.09
			HM	416.53	$\times10^{10}$ 3.8321 $\times10^{15}$	0.0417	406.38	355.51	0.982	0.16
(E)	565-1003	508	CR	117.32	3.62×10^{9}	-0.0664	113.09	146.81	0.99	0.11
			HM	119.89	1.98×10^{10}	-0.0522	115.67	142.20	0.99	0.12
(F)	304-566	493	CR	68.67	1.27×10^{5}	-0.1513	64.57	139.17	0.997	0.07
			HM	85.48	8.04×10^{6}	-0.1169	81.38	139.00	0.994	0.09

a = correlation coefficients of the Arrhenius plots and b = standard deviation.

The kinetic studies

Thermal behavior of H_2L and its complexes in terms of stability ranges, peak temperatures and values of kinetic parameters, are shown in Table 3.

The kinetic parameters have been evaluated using the following method: *Coats-Redfern equation* [37] The *Coats-Redfern* equation (1), which is a typical integral method, can be represented as:

$$\int_0^{\alpha} \frac{d\alpha}{(1-\alpha)^n} = \frac{A}{\varphi}\int_{T1}^{T2} \exp\left(\frac{-E^*}{RT}\right) dT \quad (1)$$

For convenience of integration, the lower limit T_1 is usually taken as zero. This equation on integration gives:

$$\ln\left[\frac{-\ln(1-\alpha)}{T^2}\right] = \frac{-E^*}{RT} + \ln\left[\frac{AR}{\varphi E^*}\right] \quad (2)$$

A plot of left-hand side (LHS) against $1/T$ was drawn, E* is the energy of activation in kJ mol^{-1} and calculated from the slope and A in (s^{-1}) from the intercept. The entropy of activation ΔS* in (kJ $K^{-1}mol^{-1}$) was calculated by using equation (3):

$$\Delta S^* = R \ln\left(\frac{Ah}{K_B T_s}\right) \quad (3)$$

where K_B is the Boltzmann constant, h is the Plank's constant and T_s is the DTG peak temperature.

Horowitz-Metzger equation [38]

The *Horowitz-Metzger* equation is an illustrative of the approximation methods. These authors derived the relation:

$$\log\left[\frac{\{1-(1-\alpha)^{1-n}\}}{(1-n)}\right] = \frac{E^*\theta}{2.303RT_s^2} \quad \text{for } n \neq 1 \quad (4)$$

when n = 1, the LHS of equation 4 would be log[-log (1-α)]. For a first-order kinetic process the *Horowitz-Metzger* equation may be written in the form:

$$\log\left[\log\left(\frac{w_\alpha}{w_\gamma}\right)\right] = \frac{E^*\theta}{2.303RT_s^2} - \log 2.303 \quad (5)$$

where $\theta = T-T_s$, $w_\gamma = w_\alpha - w$, w_α = mass loss at the completion of the reaction; w = mass loss up to time t. The plot of $\log[\log(w_\alpha/w_\gamma)]$ versus θ was drawn and found to be linear from the slope of which E^* was calculated. The pre-exponential factor, A, was calculated from the equation:

$$\frac{E^*\theta}{RT_s^2} = \frac{A}{\left[\varphi \exp\left(-\frac{E^*}{RT_s}\right)\right]} \quad (6)$$

The entropy of activation, ΔS^*, was calculated from equation (3). The enthalpy of activation, ΔH^*, and Gibbs free energy, ΔG^*, were calculated from;

$$\Delta H^* = E^* - RT \quad (7)$$

and

$$\Delta G^* = \Delta H^* - T\Delta S^* \quad (8)$$

It is clear that the thermal degradation process of the complexes spot that the complexes are thermally steady. The positive ΔH* values assumptions an endothermic nature of the formed complexes. These results showing a perfect fit with linear function. The negative value of ΔS* for some of the degradation steps points that the activated fragments have a more arranged structure [39]. The greater positive values of E^* point that the processes involving in translational, rotational, vibrational states and a changes in mechanical potential energy for complexes.

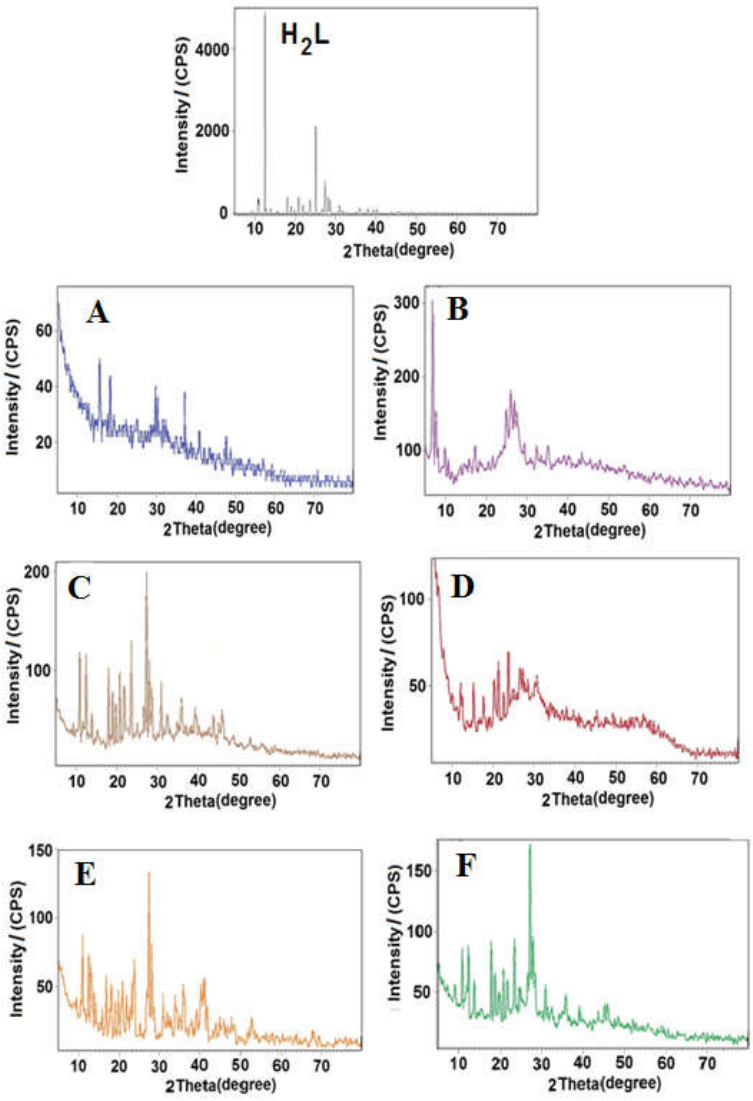

Figure 6. Powder XRD pattern for H_2L and its metal complexes.

X-ray diffraction

The X-ray diffraction method is a tool to distinguish crystalline from non-crystalline (amorphous) materials and give information about unit cell structure, lattice parameters and Miller indices. Generally, the sharp, narrow and intense peaks point the high purity and crystallinity [40]. The crystal structures of the prepared compounds H_2L, **(A)**, **(B), (C)**, **(D)**, **(E)** and **(F)** were characterized by X- ray diffraction and recorded over the scanning range 2θ = 10-70^o (Figure 6). The diffraction of H_2L, exhibited three diffraction peaks at 2θ [d value A°] = 12.49 [7.09], 25.07 [3.55] and 27.35 [3.26]. The diffractogram of complex **(A)**, indicated main peaks at 2θ [d value A°] = 15.69 [5.65], 18.35 [4.83], 29.81 [2.99], 30.40 [2.94], 37.24 [2.41], 40.96 [2.20] and 47.73 [1.91]. The XRD patterns of complex **(B)**, exhibited peaks corresponding to 2θ [d value A°] = 6.85 [12.90], 7.59 [11.63], 17.30 [5.12], 24.87 [3.58], 25.94 [3.44] and 26.85 [3.32]. The X-ray powder diffraction for complex **(C)**, gives peaks at 2θ [d value A°] = 10.89 [8.12], 12.46 [7.11], 13.89 [6.38], 17.98 [4.93], 18.95 [4.68], 19.77 [3.12], 20.78 [4.49], 21.84 [4.28], 23.60 [4.07], 27.32 [3.77], 27.99 [3.26], 28.61 [3.19] and 30.97 [2.89]. The diffraction complex **(D)**, gives peaks at 2θ [d value A°] = 12.09 [7.32], 15.18 [5.84], 17.66 [5.02], 20.23 [4.39], 21.26 [4.18], 22.61 [3.93), 23.74 [3.75] and 26.58 [3.35]. The XRD patterns of complex **(E)**, gives peaks at 2θ [d value A°] = 10.88 [8.13], 12.44 [7.11], 13.02 [6.80], 13.90 [6.37], 16.65 [5.32], 17.97 [4.94], 18.95 [4.68], 19.76 [4.49], 20.51 [4.33], 20.77 [4.28], 23.62 [3.77], 27.28 [3.27], 27.98 [3.19], 30.95 [2.89] and 35.76 [2.51]. The XRD patterns of complex **(F)**, gives peaks at 2θ [d value A°] = 10.89 [8.13], 12.42 [7.13], 13.89 [6.37], 17.98 [4.93], 18.89 [4.67], 20.76^o [4.28], 23.57 [3.77], 27.27 [3.27], 27.98 [3.19] and 30.94 [2.89]. The average crystalline size (t) of the samples of compounds was estimated from XRD data using the simple Debye-Scherer equation [41]: Where, t is the crystallite size in (nm), k is a constant dependent on crystallite shape equals to 0.89, λ is the wavelength of X–rays equals to 0.1542 nm, θ is the diffraction angle in (degree) and β is the full diffraction peak width at half maximum intensity (FWHM) in (radians).

$$\mathbf{t} = \frac{K.\lambda}{\beta.\ Cos\ \theta}$$

Nematicidal activity

The effect of H_2L and its complexes on migration of second stage larvae of root knot nematode *Meloidogyne javanica* under Laboratory conditions was studied. The data indicated that, the complexes showed a low inhibition percentage (%I) compared with H_2L. The inhibition percentage decreased from 62.5% in case of H_2L to 31.8, 26.6, 24.6 and 0 in case of La(III), Cu(II), Y(III) and Co(II) complexes, respectively. With another point of view the nematicidal effect of ligand changed to stimulation effect in case of Zr(IV) and U(VI) that increased migration (activation) of nematode by 22.7 and 15.5% up on control.

CONCLUSIONS

Metal complexes of Co(II), Cu(II), Y(III), Zr(IV), La(III) and U(VI) with H_2L ligand were formed in 1:1 molar ratio and then distinguished by different spectroscopic analyses. The prepared Schiff-bases are tetradentate where metal is bonded through -OH and azomethine C=N and forming five and six membered ring coordinate complexes. Conductivity measurements exhibited the electrolytic kind of the complexes. Thermal degradation of the complexes confirmed the proposed structures, showing the leaving of water of crystallization followed by coordination sphere decomposition. The mechanism of thermal degradation was stated.

Nematicidal activity of the complexes was evaluated and showed that (D) and (F) complexes increased migration (activation) of nematode.

REFERENCES

1. Castagnone-Sereno, P. Genetic variability in parthenogenetic root-knot nematodes, Meloidogyne spp., and their ability to overcome plant resistance genes. *Nematologica* **2002**, 4, 605-608.
2. Partida-Martinez, L.P.; Hertweck, C. Pathogenic fungus harbours endosymbiotic bacteria for toxin production. *Nature* **2005**, 437, 884-888.
3. Barbary, A.; Djian-Caporalino, C.; Palloix, A.; Castagnone-Sereno, P. Host genetic resistance to root-knot nematodes, Meloidogyne spp., in Solanaceae: From genes to the field. *Pest Manag. Sci*. **2015**, 71, 1591-1598.
4. Janssen, T.; Karssen, G.; Topalović, O.; Coyne, D.; Bert, W. Integrative taxonomy of root-knot nematodes reveals multiple independent origins of mitotic parthenogenesis. PLoS ONE **2017**, 12, e0172190.
5. Lamberth, C.; Jeanmart, S.; Luksch, T.; Plant, A. Current challenges and trends in the discovery of agrochemicals. *Science* **2013**, 341, 742-746.
6. Adekunle, O.K.; Akinlua, A. Nematicidal effects of *Leucaena leucocephala* and *Gliricidia sepium* extracts on Meloidogyne incognita infecting okra. *Nematicidal. J. Agr. Sci.* **2007**, 52, 53-63.
7. Jain, M.; Gaur, S.; Singh, V.P.; Singh, R.V. Organosilicon(IV) and organotin(IV) complexes as biocides and nematicides: Synthetic, spectroscopic and biological studies of N,N donor sulfonamide imine and its chelates. *Appl. Organomet. Chem.* **2004**, 18, 73-82.
8. Kavitha, P.; Chary, M.R.; Singavarapu, B.V.V.A.; Reddy, K.L. Synthesis, characterization, biological activity and DNA cleavage studies of tridentate Schiff bases and their Co(II) complexes. *J. Saudi Chem. Soc.* **2016**, 20, 69-80.
9. Osman, A.H. Synthesis and characterization of cobalt(II) and nickel(II) complexes of some Schiff bases derived from 3-hydrazino-6-methyl[1,2,4] triazin-5(4H)one. *Transit. Met. Chem.* **2006**, 31, 35-41.
10. Shibuya, Y.Y.; Nabari, K.; Kondo, M.; Yasue, S.; Maeeda, K.; Uchida, F.; Kawaguchi, H. The copper(II) complex with two didentate Schiff base ligands. The unique rearrangment that proceeds under alcohol vapor in the solid state to construct noninclusion structure. *Chem. Lett.* **2008**, 37, 78-79.
11. Abd El-Wahab, Z.H.; Mashaly, M.M.; Salman, A.A.; El-Shetary, B.A.; Faheim, A.A. Co(II), Ce(III) and UO_2(VI) bis-salicylatothiosemicarbazide complexes: Binary and ternary complexes, thermal studies and antimicrobial activity. *Spectrochim. Acta A* **2004**, 60, 2861-2873.
12. Ahmed, F.M.; Sadeek, S.A.; El-Shwiniy, W.H. Synthesis, spectroscopic studies, and biological activity of some new N_2O_2 tetradentate Schiff base metal complexes. *Russ. J. Gen. Chem.* **2019**, 89, 1874-1883.
13. Sadeek, S.A.; Mohamed, A.A.; El-Sayed, H.A.; El-Attar, M.S. Spectroscopic characterization, thermogravimetric and antimicrobial studies of some new metal complexes derived from4-(4-isopropyl phenyl)-2-oxo-6-phenyl-1,2-dihyropyridine-3-carbonitrile (L). *App. Organomet. Chem.* **2020**, 34, e5334.
14. El-Attar, M.S.; Abd El-Lattif, N.S.; Sadeek, S.A. Study on the nematicidal activity and chemical structure of NO bidentate Schiff base some metal complexes. *J. Chin. Chem. Soc.* **2020**, 67, 610-622.
15. Saddam Hossain, M.D.; Zakaria, C.M.; Kudrat-E-Zahan, M.D.; Zaman, B. Synthesis, spectral and thermal characterization of Cu(II) complexes with two new Schiff base ligand towards potential biological application. *Der Chemica Sinica* **2017**, 8, 380-392.

16. Addabbo, T.D.; Argentieri, M.P.; Żuchowski, J.; Biazzi, E.; Tava, A.; Oleszek, W.; Avato, P. Activity of saponins from *Medicago* species against phytoparasitic nematodes. *Plants* **2020**, 9, 443.
17. Geary, W.J. The use of conductivity measurements in organic solvents for the characterisation of coordination compounds. *Coord. Chem. Rev.* **1971**, 7, 81-122.
18. El-Jouad, E.M.; Riou, A.; Allain, M.; Khan, M.A.; Bouet, G.M. Synthesis, structural and spectral studies of 5-methyl 2-furaldehyde thiosemicarbazone and its Co, Ni, Cu and Cd complexes. *Polyhedron* **2001**, 20, 67-74.
19. Fahmi, N.; Gupta, I.J.; Singh, R.V. Sulfur bonded palladium(II) and platinum(II) complexes of biologically potent thioamides. *Phosphorus Sulfur Silicon* **1998**, 132, 1-8.
20. Rodney, P.F.; Nakayama-Ratchford, N.; Dai, H.; Lippard, S.J. Soluble single-walled carbon nanotubes as longboat delivery systems for platinum(IV) anticancer drug design. *J. Am. Chem. Soc.* **2007**, 129, 8438-8439.
21. Efthimiadou, E.K.; Katsarou, M.; Sanakis, Y.; Raptopoulou, C.P.; Karaliota, A.; Katsaros, N.; Psomas, G. Neutral and cationic mononuclear copper(II) complexes with enrofloxacin: Structure and biological activity. *J. Inorg. Biochem.* **2006**, 100, 1378-1388.
22. Sadeek, S.A.; EL-Shwiniy, W.H.; Zordok, W.A.; EL-Didamony, A.M. Spectroscopic, structure and antimicrobial activity of new Y(III) and Zr(IV) ciprofloxacin. *Spectrochim. Acta A* **2011**, 78, 854-867.
23. Sadeek S.A.; El-Attar M.S.; Abd El-Hamid S.M. Preparation and characterization of new tetradentate Schiff base metal complexes and biological activity evaluation. *J. Mol. Struct.***2013**, 1051, 30-40.
24. El-Shwiniy, W.H.; Sadeek, S.A. Synthesis and characterization of new 2-cyano-2-(*p*-tolyl-hydrazono)-thioacetamide metal complexes and a study on their antimicrobial activities. *Spectrochim. Acta A* **2015**, 137, 535-546.
25. Arif, M.; Qurashi, M.M.R.; Shad, M.A. Metal-based antibacterial agents: Synthesis, characterization, and in vitro biological evaluation of cefixime-derived Schiff bases and their complexes with Zn(II), Cu(II), Ni(II), and Co(II). *J. Coord. Chem.* **2011**, 64, 1914-1930.
26. Nour, E.M.; AL-Kority, A.M.; Sadeek, S.A.; Teleb, S.M. Synthesis and spectroscopic studies of NN-O-phenylenebis (salicylideneiminato) dioxouranium (VI) solvates (L) CL = DMF and PY). *Synth. React. Inorg. Met.-Org. Chem.* **1993**, 23, 39-52.
27. Sadeek, S.A.; EL-Shwiniy, W.H. Preparation, structure and microbial evaluation of metal complexes of the second generation quinolone antibacterial drug lomefloxacin. *J. Mol. Struct.* **2010**, 981, 130-138.
28. Mcglynn, S.P.; Smith, J.K. The electronic structure, spectra, and magnetic properties of actinyl ions: Part I. The uranyl ion. *J. Mol. Spect.* **1961**, 6, 164-187.
29. Jones, L.H. Determination of U-O bond distance in uranyl complexes from their infrared spectra. *Spectrochim. Acta A* **1959**, 15, 409-411.
30. Mondal, N.; Dey, D.K.; Mitra, S.; Malik, K.M.A. Synthesis and structural characterization of mixed ligand η1-2-hydroxyacetophenone complexes of cobalt(III). *Polyhedron* **2000**, 19, 2707-2711.
31. Refat, M.S. Synthesis and characterization of norfloxacin-transition metal complexes (group 11, IB): Spectroscopic, thermal, kinetic measurements and biological activity. *Spectrochim. Acta A* **2007**, 68, 1393-1405.
32. Psomas, G.; Tarushi, A.; Efthimiadou, E.K. Synthesis, characterization and DNA-binding of the mononuclear dioxouranium(VI) complex with ciprofloxacin. *Polyhedron* **2008**, 27, 133-138.
33. Masoud, M.S.; Ali, A.E.; Elasala, G.S. Synthesis, spectral, computational and thermal analysis studies of metallocefotaxime antibiotics. *Spectrochim. Acta A* **2015**, 149, 363-377.
34. Masoud, M.S.; Zaki, Z.M. Synthesis and characterization of 5-(arylazo)thiobarbituric acids and their complexes. *Trans. Met. Chem.* **1988**, 13, 321-327.

35. Macias, B.; Martinez, M.; Sanchez, A.; Dominguez, A. A physico-chemical study of the interaction of ciprofloxacin and ofloxacin with polivaientcations. *Int. J. Pharm.* **1994**, 106, 229-235.
36. Skauge, T.; Turel, I.; Sletten, E. Interaction between ciprofloxacin and DNA mediated by Mg^{2+} ions. *Inorg.Chim. Acta* **2002**, 339, 239-247.
37. Coats, A.W.; Redfern, J.P. Kinetic parameters from thermogravimetric data. *Nature* **1964**, 201, 68-69.
38. Horowitz, H.H.; Metzger, G. A new analysis of thermogravimetric traces. *Anal. Chem.* **1963**, 35, 1464-1468.
39. Guzar, S.H.; Jin, Q.H. Simple, selective, and sensitive spectrophotometric method for determination of trace amounts of nickel(II), copper(II), cobalt(II), and iron(III) with a novel reagent 2-pyridine carboxaldehydeisonicotinylhydrazone. *Chem. Res. Chin. Univ.* **2008**, 24, 143-147.
40. Zhao, Q.; Shen, Y.; Ji, M.; Zhang, L.; Jiang, T.; Li, C. Effect of carbon nanotube addition on friction coefficient of nanotubes/hydroxyapatite composites. *J. Ind. Eng. Chem.* **2014**, 20, 544-548.
41. Quan, C.X.; Bin, L.H.; Bang, G.G. Preparation of nanometer crystalline TiO_2 with high photo-catalytic activity by pyrolysis of titanyl organic compounds and photo-catalytic mechanism. *Mater. Chem. Phys.* **2005**, 91, 317-324.